Characterization of Natural and Affected Environments

Environmentally persistent free radical (EPFR) formation by visible-light illumination of the organic matter in atmospheric particles

Qingcai Chen, Haoyao Sun, Mamin Wang, Yuqin Wang, Lixin Zhang, and Yuemei Han

Just Accepted

1 # Environmentally persistent free radical (EPFR) formation

2 # by visible-light illumination of the organic matter in

3 # atmospheric particles

4 *Qingcai Chen,[a,*,#] Haoyao Sun,[a,#] Mamin Wang,[a] Yuqin Wang,[a] Lixin Zhang,[a] Yuemei*

5 *Han[b,c]*

6 *[a] School of Environmental Science and Engineering, Shaanxi University of Science and*

7 *Technology, Xi'an 710021, China*

8 *[b] Key Laboratory of Aerosol Chemistry and Physics, State Key Laboratory of Loess and*

9 *Quaternary Geology, Institute of Earth Environment, Chinese Academy of Sciences, Xi'an 710061,*

10 *China*

11 *[c] School of Engineering and Applied Sciences, Harvard University, Cambridge, Massachusetts*

12 *02138, United States*

13 *Corresponding author e-mail: chenqingcai@sust.edu.cn;*

14 *Phone/fax: (+86) 029-86132765;*

15 *Address: School of Environmental Science and Engineering, Shaanxi University of*

16 *Science and Technology, Weiyang District, Xi'an, Shaanxi, 710021, China*

ABSTRACT: A secondary process may be an important source of environmentally persistent free radicals (EPFRs) in atmospheric particulates, yet this process has remained to be elucidated. This study demonstrated that secondary EPFRs could be generated by visible-light illumination of atmospheric particulate matter (PM), and their lifetimes were only 30 min to 1 day, which were much shorter than the lifetimes of the original EPFRs in PM. The yields of secondary EPFRs produced by PM could reach 15% - 60% of those of the original EPFRs. The extractable organic matter contributed to the formation of secondary EPFRs (~55%), and a humic-like substance was the main precursor of the secondary EPFRs and was also the most productive precursor compared to the other aerosol components. The results of simulation experiments showed that the secondary EPFRs generated by the extractable and nonextractable PM components were similar to those produced by phenolic compounds and polycyclic aromatic hydrocarbons, respectively. We have found that oxygen molecules play an important role in the photochemical generation and decay of EPFRs. Reactive oxygen capture experiments showed that the original EPFRs may contribute to singlet oxygen generation, while the secondary EPFRs generated by photoexcitation may not produce singlet oxygen or hydroxyl radicals.

Key words: $PM_{2.5}$, Secondary EPFRs, Sources, Formation Mechanism

TOC/Abstract Art
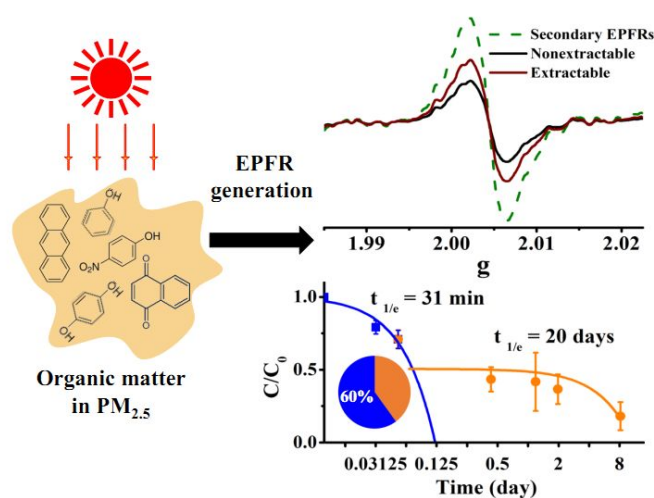
1. INTRODUCTION

Environmentally persistent free radicals (EPFRs) are environmentally hazardous substances with longer lifetimes (up to months and years) compared to traditional short-lived free radicals (such as hydroxyl radicals ($\cdot$OH) and superoxide radicals).[1-4] EPFRs were first discovered in cigarette tar and are considered to be semiquinones.[5,6] In recent years, studies have found the presence of EPFRs in soils, fly ash and atmospheric particulates.[7-9] Studies have found that EPFRs can catalyze the production of reactive oxygen species (ROS) by oxygen molecules, which may cause damage to lung cells.[10-14]

In recent years, scholars have gradually increased the research on the sources and formation mechanisms of EPFRs in atmospheric particulate matter (PM). PM EPFRs can originate from both primary and secondary sources. Yang et al. found that coal combustion and traffic source particles contain large amounts of EPFRs.[15] Wang et al. also found that the suspended particles produced by coal combustion contain large amounts of EPFRs and predicted that coal combustion may be an important source of EPFRs in atmospheric PM in the Xuanwei area.[16] The EPFRs in a primary combustion source were certain phenoxy or semiquinone free radicals, which were thought to be mainly formed by the action of metal oxides (such as Fe_2O_3 and CuO) and aromatic substances under high-temperature conditions.[17-24] Dust can also contribute to atmospheric EPFRs. Chen et al. found that Asian dust storms can increase the atmospheric EPFR concentration levels and transmit EPFRs over long distances.[25] In addition to the primary source, atmospheric EPFRs may also form through a secondary chemical process in the atmosphere. Chen et al. found that the concentrations of EPFRs in fine particulate matter ($PM_{2.5}$) in summer in Xi'an were highly correlated with the concentrations of O_3, thereby indicating that certain EPFRs may be related to atmospheric oxidation processes.[26] The oxidation of polycyclic aromatic hydrocarbons (PAHs) by O_3 to form EPFRs has been confirmed under laboratory conditions, and different PAH precursors can generate different types of EPFRs.[27] Tong et al.'s laboratory study of secondary organic aerosol (SOA)

3 / 28

generation found that the aerosols produced by PAHs contained EPFRs.[28] PAHs have also been identified as important precursors for the production of EPFRs by photochemical reactions; the degradation of anthracene and pyrene on clay particles produced many EPFRs that lasted longer than one month.[16] Throughout the current research on the secondary generation mechanism of EPFRs, the mechanism has been found only under laboratory simulation conditions, and most of the research objects are PAHs; furthermore, there are few studies on ambient PM. However, ambient atmospheric particulates contain thousands of compounds. The secondary formation mechanism and physicochemical properties of EPFRs in ambient PM may be more complicated.

To understand the characteristics and mechanisms of the photochemical generation of EPFRs in atmospheric PM, in this study, the dynamics, types, decays and relative contributions of photochemically generated EPFRs in atmospheric $PM_{2.5}$ samples and their different components were systematically studied using an electron paramagnetic resonance spectrometer (EPR). The characteristics of the secondary EPFRs of different PM compounds were also compared, and the possible formation mechanism of secondary EPFRs was discussed. Finally, this study also explored the possibility of generating ROS in secondary EPFRs. The most important conclusion of this study was to demonstrate that atmospheric photochemistry was an important route for the secondary generation of EPFRs in atmospheric PM and that the main precursor for the generation of secondary EPFRs was the humic-like substance (HULIS) component. The results of this study are of great significance for a comprehensive and in-depth understanding of the sources and health effects of EPFRs in atmospheric PM.

2. EXPERIMENTAL SECTION

2.1. Experimental Materials. A Mn^{2+} standard in ZnS and Cr^{3+} standard in MgO were purchased from Freiberg Instruments Inc., Delfter, Germany, and used to correct the *g*-factors and absolute spin numbers of the samples. Glucose (GC purity, $\geq 99.5\%$),

94 1,4-naphthoquinone (AR purity, $\geq$ 97.5%), hydroquinone (GC purity, $\geq$ 99.5%),

95 2-methyl-4-nitrophenol (GC purity, $\geq$ 99%), o-nitrophenol (GC purity, $\geq$ 99.7%) and

96 2,2,6,6-tetramethylpiperidine (TEMP) (GC purity, $\geq$ 98%) were purchased from the

97 Aladdin Reagent Company (Shanghai, China). Resorcinol (AR purity, $\geq$ 97.5%),

98 anthracene (GC purity, $\geq$ 99.7%) and pyrene (GC purity, $\geq$ 99%) were purchased from

99 the Macklin Reagent Company (Shanghai, China). High-purity graphite and graphene

100 oxide (GO) were purchased from Shandong Jin Cheng Graphene Technology Co., Ltd.

101 (Beijing, China). A Cleanert C18 cartridge (500 mg/6 mL, Agela, China) was used to

102 separate the HULIS from the aqueous extracts of $PM_{2.5}$ samples.

103 5-Tert-butoxycarbonyl 5-methyl-1-pyrroline N-oxide (BMPO) (GC purity, $\geq$ 99%,

104 Dojindo Company, Shanghai, China) was used to detect ·OH.

105 **2.2. Sample Collection.** A high-volume sampler (XT-1025, Shanghai Xintuo,

106 China) was used to collect $PM_{2.5}$ samples at the Shaanxi University of Science and

107 Technology, Weiyang District, Xi'an, China. Each sample collection started at 7:00

108 local time, collection lasted 23.5 h, and the sampling flow rate was 1000 L/min.

109 Samples were collected on a baked (450°C, 6 h) quartz filter (2500 QAT-UP, Pallflex

110 Products Co., US), and the samples were stored at - 20°C until testing. A total of 23

111 real atmospheric $PM_{2.5}$ samples were used for the study. To analyze the effects of

112 visible light on real samples, particulates were collected in spring (April 6-8, 2018; n

113 = 3), summer (July 10-12, 2018; n = 3), autumn (October 10-12, 2017; n = 3), and

114 winter (December 27-29, 2017; n = 3), and a dust sample (atmospheric $PM_{2.5}$; April

115 10-11, 2018; n = 2) was collected during a sandstorm; the PM_{10} concentrations on

116 April 10 and 11, 2018, were 328 μg/m^3 and 359 μg/m^3 (http://www.cnemc.cn/). The

117 samples used for solvent extraction were the 12 samples from December 1 to 13,

118 2017.

119 **2.3. Sample Preparation.** Methanol-soluble organic matter (MSOM), HULIS and

120 high-polarity water-soluble organic matter (HP-WSOM) were prepared for the EPFR

121 photochemical secondary generation experiments. Two 9 mm PM quartz filters were

122 placed in a 12 ml glass bottle, and 3 ml of methanol or ultrapure water was added and

123   vortexed for 5 min; then, the suspension was filtered with a 45 mm

124   polytetrafluoroethylene (PTFE) filter to obtain MSOM and WSOM. The WSOM was

125   separated into the HULIS and HP-WSOM by a C18 cartridge. The specific method is

126   referenced from another study.[29] Finally, the MSOM, HULIS and HP-WSOM were

127   concentrated to 0.1 ml with N_2.

128   To explore the possible mechanism by which atmospheric PM generates EPFRs

129   under visible-light conditions, MSOM; HULIS; HP-WSOM; and 10 mg/ml phenol,

130   hydroquinone, resorcinol, o-nitrophenol, 2-methyl-4-nitrophenol, 1,4-naphthoquinone,

131   and pyrene in methanol and anthracene solution of benzene were added dropwise to a

132   5 × 28 mm blank quartz filter. A rotary evaporator (Dragon RE100-Pro, Beijing,

133   China) was used to completely evaporate the solvent to be excited by light.

134   The procedure for separating the nonextractable components in the PM samples

135   was described in Chen et al.[29] Briefly, the quartz filter with $PM_{2.5}$ attached was cut

136   into two 50 mm diameter disks, and the samples were stacked on one side and placed

137   in a special filter. Then, the sample was rinsed with water, methanol, dichloromethane,

138   n-hexane, 10 ml each time and filtered three times. After the filtration was completed,

139   the filter was placed in a rotary evaporator to completely evaporate the solvent

140   remaining on the filter to obtain a sample of the nonextractable components

141   containing black carbon. Chen et al. demonstrated that nonextractable components

142   were the main contributors (over 80%) of EPFRs in atmospheric $PM_{2.5}$.[29] Our

143   previous studies have shown that this process has little effect on the original EPFRs.[29]

144   **2.4. EPR Measurements and Data Analysis.** Quartz filters were placed in quartz

145   tissue cells and detected by an EPR (MS5000, FREIBERG, Germany). Specific test

146   methods have been discussed in published papers.[30] The EPR parameters were set to

147   magnetic field strength, 335 - 342 mT; detection time, 60 s; modulation amplitude,

148   0.20000 mT; number of detections, 1; and microwave intensity, 8.0 mW. The

149   parameters of the online and offline detection methods were the same.

150   To calculate the lifetimes of the different types of EPFRs, we calculated the

151   lifetimes using the following formula:[26]

152          $\ln(C/C_0) = -kt$ (1)

153          $t_{1/e} = 1/k$ (2)

154   where C_0 and C are the initial semaphores of the EPFRs in the sample and the

155   semaphores after decay time t, respectively, and k is the rate constant derived from the

156   logarithmic slope of the radical semaphore ratio (C/C_0) versus time, which results in

157    $t_{1/e}$.

158   **2.5. Visible-light excitation.** The visible-light excitation experiment used a

159   Hamamatsu lamp (E1502 - 04, Optical Stimulation Unit, Japan) as the light source

160   (visible light: 400 ~ 700 nm), and the light source power was 2.0 W/cm^2. Directly

161   illuminating the filter with $PM_{2.5}$ or other attached components, the filter receiving

162   power was approximately 3 W, and the temperature and humidity under light

163   conditions were approximately 45°C and 25%, respectively. The light source was

164   connected with the EPR to perform the process of detecting the generation of EPFRs

165   online. Offline detection consisted of directly illuminating the sample with the light

166   source for 10 min and then rapidly putting the sample into the EPR to detect the

167   amounts of EPFRs generated.

168   **2.6 Organic carbon (OC)/elemental carbon (EC) analysis.** The contents of

169   organic carbon (OC) and elemental carbon (EC) in the sample were quantified using a

170   multiband OC/EC analyzer (DRI, Model 2001A) using the IMPROVE_ A detection

171   method. The sample was placed in a 100% pure helium atmosphere and heated in four

172   stages at 140°C (OC1), 280°C (OC2), 480°C (OC3) and 580°C (OC4) to pyrolyze the

173   OC material. Then, in a 2% oxygen and 98% helium atmosphere, the EC was heated

174   in three stages: 580°C (EC1), 740°C (EC2) and 840°C (EC3). The carbon dioxide

175   produced at each temperature gradient was detected by a nondispersive infrared

176   (NDIR) detector. The pyrolyzed organic carbon (CPor) was monitored with 632 nm

177   reflected light; finally, OC = OC1 + OC2 + OC3 + OC4 - CPor, EC = EC1 + EC2 +

178   EC3.

179   **2.7 Active oxygen detection.** To detect the ability of the secondary EPFRs to

180   generate singlet oxygen ($^1O_2$) and ·OH, two 9 mm quartz membranes with $PM_{2.5}$

181   attached were obtained, exposed to visible light for 10 min, and rapidly placed in a

182   centrifuge tube, and 0.2 ml of a 100 mM TEMP and BMPO solutions were

183   respectively added in duplicate samples to capture $^1O_2$ and $\cdot OH$. Then, a vortex

184   shaker (MX-S, SCILOGEX, USA) was used to oscillate for 5 min, and 0.03 ml of the

185   suspension was placed into a capillary and placed in the EPR to detect ROS. The

186   nonilluminated sample and the water-soluble substance were treated the same as in

187   the detection method.

188   The EPR detection parameters for the $^1O_2$ and $\cdot OH$ are the same: magnetic field

189   strength, 330 - 342 mT; detection time, 180 s; modulation amplitude, 0.20000 mT;

190   number of detections, 1; and microwave intensity, 8.0 mW.

191   ## 3. RESULTS AND DISCUSSION

192   **3.1 Visible light stimulates PM to generate EPFRs.** This study demonstrated that

193   EPFRs can be generated by the visible-light excitation of atmospheric $PM_{2.5}$ samples.

194   As shown in Figure 1a, the $PM_{2.5}$ sample showed a significant enhancement in the

195   EPR signal after being exposed to visible light, indicating that secondary EPFRs were

196   formed by the excitation of the real atmospheric $PM_{2.5}$ sample by visible light. The

197   change in the EPR signal intensity in the experiment may also be affected by the

198   ambient temperature and humidity. We eliminated the influences of environmental

199   conditions on the determination of EPFRs in the sample by adding verification

200   experiments (Figure S1).

201   The increases in the EPFR contents in different $PM_{2.5}$ samples were different. As

202   shown in Figure 2a, the spring, summer, and autumn samples increased by 1.15 - 1.25

203   times, while the winter sample increased by 1.6 times that of the original EPFR

204   content. This result means that the photochemical formations of EPFRs depend on the

205   chemical composition of the PM, and the winter samples may contain more

206   components that can generate EPFRs by photochemical action. Spring in Xi'an is a

207   season during which sandstorms often occur. The concentrations of EPFRs in $PM_{2.5}$ in

208   dust weather will increase significantly and can be transmitted over long distances.[25]

209   However, this study found that the EPFR signal was not significantly enhanced by

210   visible-light illumination (only approximately 1.1 times higher), indicating that there

211   are not large amounts of components in the dust particles that can be excited by

212   visible light to cause EPFRs to be generated.

213   The types of secondary EPFRs generated in the $PM_{2.5}$ samples excited by light

214   were different from the EPFRs in the original filter. As shown in Figure 2b, the

215   g-factors of the EPFRs increased by 0.002 - 0.004 after illumination, indicating that

216   the EPFRs generated under light conditions have higher g-factors, which is

217   significantly different from the EPFRs contained in the original samples. To

218   investigate whether EPFRs can continuously be generated in PM samples by

219   illumination, the same sample was repeatedly illuminated three times. As shown in

220   Figure 2b, the results show that EPFRs can be generated during each illumination, and

221   the amount of generation and g-factor were the same each time. The results indicate

222   that the generation of EPFRs was reproducible, and the precursors of the EPFRs that

223   can be generated in PM are not consumed with the increase in the illumination time

224   under visible-light illumination.

225   We studied the kinetics of the photochemical generation and decay of EPFRs.

226   Figure 1b shows the relative concentrations of EPFRs over time during continuous

227   illumination of the PM samples (the spring, summer, and autumn samples can refer to

228   Figure S2, S3). The increasing trends of the EPFRs after exposure to light can be

229   roughly divided into three stages: the EPFR content increased rapidly during the first

230   1 min; then, the rate of increase gradually slowed down within 1-7 min; finally, the

231   EPFR content stabilized until approximately 7 min. When the illumination stopped,

232   the EPFRs showed a rapid decay tendency (within 1 min), after which the decay rate

233   slowed, and the EPFR content decreased to the initial level within 1 day. This rapid

234   decay indicates that the secondary generated EPFRs are chemically unstable. As

235   shown in Figure 1c, the variations in the g-factors of the EPFRs are slightly different

236   from the trend of the EPFR concentration. The g-factor will increase rapidly within 1

237   min of the start of illumination, while the g-factor will remain essentially unchanged

238   within 1 - 10 min. When the illumination is stopped, the g-factor will slowly decrease

239   and decrease to the *g*-factor value of the initial sample within 1 day.

240   The above results indicate that the process of photoexcitation to generate EPFRs

241   was rapid, and the generated EPFRs were unstable, which means that the short-term

242   health risks of this portion of the secondary EPFRs may be higher. This portion of the

243   secondary EPFRs was significantly different from the original EPFRs in the sample.

244   The *g*-factors of the EPFRs in the original sample were lower than those of the

245   secondary EPFRs, and the lifetimes were much longer than those of the secondary

246   EPFRs.[29] The secondary formation of EPFRs may also be included in the ambient PM

247   samples. The EPFRs in the autumn samples showed significant attenuation levels in

248   the first few days.[26] This portion of the EPFRs that were susceptible to decay may

249   contain EPFRs formed by photoexcitation in the real atmosphere. The percentages of

250   rapid decay of the EPFRs in the different seasons were different. This phenomenon

251   may be due to the different sources and chemical components of the EPFRs in

252   different seasons, resulting in different levels of EPFRs generated by light excitation.

253   There were many occurrences of dusty weather in spring, and the sand dust samples

254   were not easily excited by visible light to generate EPFRs. Most of the substances that

255   can be excited in $PM_{2.5}$ in the summer may have been decomposed by intense light

256   and other oxidants. The extreme decay of the EPFRs in the autumn samples has been

257   verified,[26] which may be related to photochemically generated EPFRs. The

258   concentrations of EPFRs in the winter samples were relatively high, but the seasonal

259   illumination was weak. The relative amounts of EPFRs generated by light in the real

260   samples were limited, so there was a large number of EPFRs generated by visible

261   light in the winter samples.

262   **3.2. Photochemical generation of EPFRs from the different components in**

263   **$PM_{2.5}$.** The above results indicate that the atmospheric PM samples contain certain

264   components that can be excited by visible light to produce EPFRs. To study which

265   components lead to the formation of EPFRs under illumination conditions, this study

266   investigated the generation of EPFRs by different polar PM components. Figure 3a

267   shows the average EPR spectra of the EPFRs produced by different PM components

268 excited by visible light. The results showed that the concentrations of EPFRs excited

269 in the washed sample were significantly lower than those of the original sample

270 (average reduction: 55%), but our previous research shows that the contents of the

271 original EPFRs in the extracted sample underwent little change (average reduction:

272 12%).[29] This finding indicates that the extractable PM components may have an

273 important contribution to the generation of secondary EPFRs. Our previous research

274 shows that MSOM contains only small amounts of original EPFRs (< 3%),[29] but after

275 exposure to visible light, large amounts of EPFRs are produced (see Figure 3a). The

276 g-factor of the EPFRs generated by MSOM was 2.0050 ± 0.0001, which was a typical

277 O-centered free radical; the result was consistent with the EPFR characteristics of the

278 photochemical secondary generation of the original sample. Similarly, the HULIS was

279 also excited by visible light to produce a large number of EPFRs, and the HULIS

280 EPFR production and g-factor (2.0051 ± 0.0001) were similar to those of the MSOM.

281 In contrast, the HP-WSOM did not produce EPFRs after being exposed to visible light.

282 The above results indicate that the HULIS in the PM samples were the most important

283 components in generating secondary EPFRs. Based on the above results, as shown in

284 Figure 3b, we conclude that the contributions of the extractable and nonextractable

285 PM components to the secondary EPFRs were 55% and 45%, respectively, while the

286 contribution rate of the HULIS in the extractable components reached 82% of the

287 total EPFR production. Because methanol can be extracted, including HULIS and

288 water-insoluble organics, it can be inferred that the methanol-extractable

289 water-insoluble organics contribute only approximately 18% of the total EPFR

290 production. To compare the abilities of different components to photochemically

291 generate EPFRs, the study used the amounts of OC in different components to

292 standardize the ability to generate EPFRs. As shown in Figure 3c, the HULIS had the

293 highest generation capability of 8×10^{13} spins/μg OC. The washed sample (2.8×10^{13}

294 spins/μg OC) and methanol-extractable water-insoluble component (1.8×10^{13}

295 spins/μg OC) followed, while the HP-WSOM did not have the ability to generate

296 EPFRs.

297 The g-factors of the EPFRs generated by photoexcitation of the MSOM and HULIS

11 / 28

298   were between 2.0048 and 2.0052, similar to those of the semiquinone-type free

299   radicals.[31] This result may be caused by certain aromatic compounds containing

300   heteroatoms excited by visible light. For example, hydroquinone, catechol and other

301   organic substances will undergo dehydrogenation under light conditions to form

302   phenoxy radicals, cyclopentadienyl and semiquinone radicals.[18] The washed filter can

303   still be photoexcited to form EPFRs, which may be formed by difficult-to-extract

304   substances containing macromolecular polyphenyl rings, such as GO-like materials.

305   Chen et al. believed that the residual substances in PM contain GO-like substances

306   and are the main EPFR contributors in the original sample,[29] while GO itself can

307   undergo photocatalytic reactions.[32] The added experiments have confirmed that

308   EPFRs are produced after GO is illuminated, and the EPFRs produced are similar to

309   those of the solvent-washed filter (Figure S5). We conclude that GO may be an

310   important contributor to the formation of EPFRs in the leaching residue.

311   **3.3. Light stimulates the reference compound to generate EPFRs.** To determine

312   which substances in $PM_{2.5}$ are excited by light to produce EPFRs, different reference

313   compounds were used to simulate EPFR generation by PM. The selection of these

314   chemical standards was based on the characteristics of the chemical components in

315   the real atmospheric sample. The reference substances and results are shown in Table

316   1 (the EPR spectrum is shown in Figure S6). The results showed that all organic

317   compounds except glucose produced EPFRs after stimulation, but the characteristics

318   of the EPFRs generated were different. The *g*-factors of phenolic substances, such as

319   phenol, nitrophenol, etc., were between 2.0048 and 2.0052, which was very consistent

320   with the EPFRs generated by extractable components (HULIS and MSOM). However,

321   the PAHs and phenolic compounds were different. The *g*-factor of the EPFRs

322   generated by anthracene and 1,4-naphthoquinone was 2.0044 - 2.0046, which was

323   similar to that reported by Tong et al.[28] The *g*-factor of the EPFRs generated by

324   pyrene was 2.0040 - 2.0042. The production of EPFRs by PAHs may be related to the

325   photolysis of PAHs. For example, anthracene was photolyzed to produce

326   9,10-anthraquinone.[33] The *g*-factor of the EPFRs produced by PAH illumination was

327   significantly lower than that of the extractable PM components, indicating that PAHs

328   were unlikely to be the main precursors of the photochemically generated EPFRs in

329   the extracted components. The formation of EPFRs in the extractable components of

330   PM was more similar to the contributions of phenolic compounds.

331   This study compared the decay characteristics of the photochemically generated

332   EPFRs from different compounds and different atmospheric PM components. Figure

333   4 shows the decay curves of the EPFRs generated by different PM extraction

334   components and different standard compounds. The decay of the EPFRs generated by

335   MSOM can be divided into two stages. The first stage is fast decay, and its $1/e$

336   lifetime was 31 min, which was approximately 63%; the second stage was slow decay,

337   and its $1/e$ lifetime was 20 days, which accounted for approximately 37%. Similarly,

338   the HULIS also had similar results to that of the MSOM (see Figure S7), and both

339   EPFRs had similar decay characteristics to those of the ambient PM sample (see

340   Figure 1b). This result reaffirms that the extractable components were the main

341   contributors in the PM samples to be excited by light to generate EPFRs. As shown in

342   Figure 4b, the decay characteristics of phenol can be divided into two stages: fast

343   decay and slower decay. The $1/e$ lifetimes were 21 min and 1 day, respectively, and

344   the ratio of both parts was 50%. Hydroquinone, resorcinol, etc. were similar (see

345   Figure S7) to the MSOM and HULIS. The decay characteristics of anthracene can be

346   divided into two stages (Figure 4c), where the $1/e$ lifetimes were 0.4 days and 39 days,

347   and the proportions of the two parts were 45% and 55%. The results for

348   1,4-naphthoquinone were very similar to those of anthracene (see Figure S5).

349   However, the results were all different from those of pyrene, and the EPFRs generated

350   by pyrene not only have no attenuation but increase in the first 5 min (approximately

351   1.2 times), after which the concentration remains unchanged (Figure 4d). This

352   phenomenon of no reduction was also observed for the water-insoluble organic matter

353   (OM) of $PM_{2.5}$, which may be attributed to the continued oxidation of the phenolic

354   functional groups leading to the formation of quinonoids in the atmosphere.[29] Based

355   on the results of the above comparative analysis, it was speculated that the substances

356   in the extractable components that can be photoexcited to generate EPFRs may be

357 mainly attributed to the phenolic substances rather than the PAHs. In contrast, the

358 formation of EPFRs by the nonextractable components was most likely caused by

359 PAHs. From the overall photochemical generation of EPFRs by PM, the contributions

360 of phenol-like substances and PAHs to the secondary formation of EPFRs were

361 similar.

362   To further clarify the mechanisms of secondary EPFR formation and decay, this

363 study investigated the effects of oxygen molecules on the formation and decay of

364 EPFRs. The MSOM was placed under N_2 and air conditions for illumination to

365 generate EPFRs. The results showed that the same number of EPFRs were generated

366 under both conditions, and the EPFRs were all oxygen-centered EPFRs (Figure S8a).

367 However, when pyrene was placed under N_2 and air conditions for illumination, the

368 amounts of EPFRs generated under N_2 conditions were reduced by 50% - 60%

369 compared to those under air conditions (Figure S8c). This result indicated that the O_2

370 molecule may be a necessary condition for the generation of secondary EPFRs.

371 However, MSOM can still generate secondary EPFRs in the absence of oxygen,

372 probably because MSOM itself contains a large number of oxygen-containing

373 functional groups,[34] which can provide the oxygen atoms required for the formation

374 of EPFRs. In contrast, PAHs do not have oxygen-containing functional groups

375 themselves, so external oxygen molecules must participate in the reaction to generate

376 secondary EPFRs. For example, the central ring of anthracene has a low *p*-orbital

377 stability, which makes the ring vulnerable to attack by O_2,[35,36] and its photooxidation

378 products anthraquinone and hydroxyanthraquinone are considered to be toxic.[37-39]

379 Similarly, the EPFRs generated by MSOM were placed under N_2 and air conditions to

380 observe the decay characteristics. The results show (Figure S8b) that the secondary

381 EPFRs in N_2 decay only 10%-20% in 45 min, which is significantly lower than when

382 exposed to air (decay ~ 60%). This result indicates that the O_2 molecule promotes the

383 decay of secondary EPFRs. We speculate that the secondary generated EPFRs may be

384 in a similar triplet excited state formed by illumination-excited OM and can transfer

385 energy to O_2 molecules to generate $^1O_2$ during decay. Generally, the triplet state of

386 OM (^{3}OM*) was 180-310 kJ/mol, which was significantly higher than the energy of

14 / 28

387     $^1O_2$ of 94 kJ/mol, so the $^3OM^*$ was fully capable of converting O_2 into $^1O_2$.[40]

388   Based on the above experimental results, we hypothesized the possible formation

389   and decay mechanisms of secondary EPFRs in atmospheric PM (Figure S9). We

390   divided the EPFR generation processes into two categories according to whether the

391   precursor contained oxygen atoms. The OM containing oxygen atoms was

392   photoexcited to generate electron transitions that formed EPFRs similar to the excited

393   condition of the triplet state. Organic substances that do not contain oxygen atoms,

394   such as PAHs, must participate in the formation of EPFRs with oxygen molecules to

395   form O-PAHs that contain oxygen atoms and then generate excited states to form

396   EPFRs. When the secondary EPFRs decay, O_2 molecules act as quenchers for the

397   EPFRs, which themselves are converted to $^1O_2$, and the EPFRs are returned to the

398   ground state. Therefore, the secondary EPFRs were prone to decay in the presence of

399   oxygen and could be repeatedly excited to produce EPFRs.

400   **3.4. Light-excited EPFRs generate ROS.** The above results indicate that the

401   secondary EPFRs were extremely unstable, indicating that secondary EPFRs may

402   have high chemical reactivities. To investigate whether photochemically generated

403   secondary EPFRs contribute to the oxidation potential of PM, this study investigated

404   the abilities of secondary EPFRs to generate $^1O_2$ and ·OH. The concentration of $^1O_2$

405   produced by the PM samples changes with time, and the $^1O_2$ concentration tends to be

406   stable at 24 h (Figure S10). As shown in Figure 5a and Figure 5b, the original filter

407   sample, the lighted filter sample and the water-soluble substance of the original filter

408   sample produced similar concentrations of $^1O_2$ in the initial 5 min. However, after 24

409   h, the $^1O_2$ concentrations produced by the original filter sample and the illuminated

410   filter sample were significantly enhanced (approximately 100% increase), but the

411   samples produced the same $^1O_2$ concentrations, while the water-soluble substance had

412   only a slight increase (increased by approximately 20%). Note that the illuminated

413   filter samples were only illuminated before the ROS capture experiment in order to

414   generate secondary EPFRs, and the ROS capture and storage process was performed

415   in dark conditions for all samples, thus avoiding the ROS generation caused by

416   illumination in the capture experiment. Since the ROS production amount and the

417   time-varying curve of the original sample and the illuminated sample are completely

418   identical, the PM that can produce $^1O_2$ mainly contained certain water-insoluble

419   substances. The EPFRs in the original filter were likely to produce $^1O_2$, and this

420   reaction process was slower than that of the active water-soluble oxidation

421   substance.[9,14] However, the secondary EPFRs generated by photochemistry did not

422   produce significant levels of $^1O_2$.

423   As shown in Figure 5c, the original sample and the illuminated sample produced

424   weaker signals of ·OH, which were significantly lower than the signal intensity

425   of ·OH (approximately 2.5 times) produced by the water-soluble substance. This

426   result indicates that water-insoluble substances, such as certain reducing organic

427   substances in PM, may quench ·OH. Comparing the signal intensities of the ·OH

428   generated by the original sample and the illuminated sample, the secondary EPFRs

429   did not produce significant ·OH. Tong et al. found that the SOAs produced from

430   naphthalene contained EPFRs but did not produce ·OH.[28] Note that this study does

431   not rule out the hydrolysis of secondary EPFRs or chemical reactions with other

432   aerosol components. This experiment does not strictly state that secondary EPFRs do

433   not have the ability to produce ROS. At present, the theory is that the health risks of

434   EPFRs are thought to be due to the interaction of EPFRs with oxygen molecules to

435   generate ROS. Combined with the results of this study, we believe that it is time to

436   thoroughly investigate whether secondary EPFRs can cause health hazards.

4. ENVIRONMENTAL IMPLICATIONS

438   In this study, we demonstrated that secondary photochemical processes may be an

439   important mechanism for the formation of short-life EPFRs in atmospheric PM. This

440   result is important for understanding the sources and formation mechanisms of

441   atmospheric EPFRs. It was generally determined that atmospheric EPFRs last at least

442   one day or longer after the collection of PM.[1,2,25] Our results indicate that previous

443   studies may have underestimated the total concentrations of EPFRs, especially in

444 seasons and regions where the light was intense. Secondary EPFRs may have decayed

445 rapidly during the sampling process. Generally, a rapid decay means that the chemical

446 reactivity is strong, and the risk of health damage should be higher.[42] Therefore, the

447 health damage of the PM samples analyzed offline may be partially underestimated.

448 Future efforts should include online monitoring of the health damage or assessment

449 methods, such as the online monitoring of atmospheric EPFRs, ROS, etc.[43]

450   This study found that the extractable OM was the main component contributing to

451 the formation of secondary EPFRs, of which the HULIS was the main contributors,

452 and their abilities to generate secondary EPFRs were stronger than those of the other

453 PM components. The facts and mechanisms of the photochemical generation of PAHs

454 have been studied in previous studies,[44-46] but the formation of EPFRs in other organic

455 components of the atmospheric PM has not been fully studied. The results of this

456 study demonstrated that the HULIS is an important secondary EPFR-forming

457 precursor in addition to the PAHs in atmospheric PM. The EPFRs generated by

458 extractable and nonextractable components may be mainly derived from phenolic

459 compounds and PAHs, respectively. This information provides important insights into

460 a deeper understanding of the secondary EPFR generation mechanism in atmospheric

461 PM.

462   This study found that O_2 plays an important role in the photochemical generation

463 and decay of EPFRs. This finding indicates that the photochemical generation of

464 EPFRs in the atmospheric PM was controlled not only by the conditions of

465 illumination but also by the transfer of O_2 from the atmosphere to the interior of the

466 particles. However, the latter does not affect the majority of the aerosol OM, such as

467 HULIS, to produce EPFRs because the OM itself can provide the oxygen atoms

468 needed for the reaction. This condition was different from the conditions needed for

469 PAHs to form EPFRs. PAHs must participate in the reaction of O_2 to form EPFRs.[16]

470 Regardless of whether the precursor contains oxygen atoms, oxygen molecules are

471 important quenchers during decay. It can be speculated that the internally contained

472 EPFRs may be more stable than the surface-distributed EPFRs,[49] which is due to the

473 lower concentrations of O_2 inside the particles. The EPFRs distributed on the surface

474 of PM can be sufficiently in contact with air to decay faster. However, for the EPFRs

475 existing inside the particles, only a small amount is quenched by O_2. Future research

476 should confirm this mechanism.

477 O_2 quenches EPFRs and may generate ROS, such as superoxide. Khachatryan's

478 research shows that PM EPFRs can convert oxygen molecules into superoxide anions,

479 which in turn generate ·OH.[14] The results of this study showed that the EPFRs in the

480 original membrane were likely to contribute to the formation of $^1O_2$. However, the

481 secondary EPFRs generated by photoexcitation did not produce large amounts of $^1O_2$

482 and ·OH. The current contradiction is not fully understood. Whether secondary

483 EPFRs have health risks requires further research in the future.

484 **ASSOCIATED CONTENT**

485 **Supporting information**

486 The supporting information contains additional details, including the EPR spectra of

487 the samples under different environmental conditions, the time-variation curves of the

488 EPFR concentration and *g*-factor in the different seasons, the relative amounts of the

489 secondary EPFRs generated by different components in the real atmospheric

490 particulates, the EPR spectra of phenolic compounds, the PAHs and GO after

491 illumination, the decay curves of the secondary EPFRs generated by the selected

492 phenolic substances and PAHs, the effects of air on the generation and decay of

493 secondary EPFRs, the generation mechanism of secondary EPFRs and the intensities

494 of the $^1O_2$ signal changes with time.

495 **Author information**

496 Corresponding Author:

497 *Q.C., phone/fax: 0086-029-86132765; e-mail: chenqingcai@sust.edu.cn.

498 Author Contributions:

499 #Q.C. and H.S. contributed equally to this work.

500 **Acknowledgments**

References

(1) Vejerano, E. P.; Rao, G.; Khachatryan, L.; Cormier, S. A.; Lomnicki, S. Environmentally persistent free radicals: Insights on a new class of pollutants. *Environ. Sci. Technol.* **2018**, 52 (5), 2468–2481.

(2) Gehling, W,; Dellinger B. Environmentally persistent free radicals and their lifetimes in PM2.5. *Environ. Sci. Technol*. **2013**, 47 (15), 8172–8178.

(3) Pryor, W. A. Oxy-Radicals and Related Species: Their Formation, Lifetimes, and Reactions. *Annu. Rev. Physiol.* **1986**, 48, 657–667.

(4) Finkelstein, E.; Rosen, G. M.; Rauckman, E. J. Production of hydroxyl radical by decomposition of superoxide spin-trapped adducts. *Mol. Pharmacol.* **1982**, 21 (2), 262–265.

(5) Ingram, D. J. E.; Tapley, J. G.; Jackson, R.; Ingram, D. J. E.; Tapley, J. G.; Jackson, R.; Bond, R. L.; Murnaghan, A. R. Paramagnetic resonance in carbonaceous solids. *Nature.* **1954**, 174 (4434), 797–798.

(6) Lyons, M. J.; Spence, J. B. Environmental free radicals. *Br. J. Cancer.* **1960**, 14 (4), 703–708.

(7) Dellinger, B.; Pryor, W. A.; Cueto, R.; Squadrito, G. L.; Hegde, V.; Deutsch, W. A. Role of free radicals in the toxicity of airborne fine particulate matter. *Chem. Res. Toxico*l. **2001**, 14 (10), 1371–1377.

(8) Truong, H.; Lomnicki, S.; Dellinger, B. Potential for misidentification of environmentally persistent free radicals as molecular pollutants in particulate matter. *Environ. Sci. Technol.* **2010**, 44 (6), 1933–1939.

(9) Vejerano, E.; Lomnicki, S.; Dellinger, B. Formation and stabilization of combustion-generated environmentally persistent free radicals on an Fe(III)2O3/silica surface. *Environ. Sci. Technol.* **2011**, 45 (2), 589–594.

(10) D'Arienzo, M.; Gamba, L.; Morazzoni, F.; Cosention, U.; Creco, C.; Lasagni, M.; Pitea, D.; Moro, G.; Cepek, C.; Butera, V.; Sicilia, E.; Russo, N.; Muñoz-García, A.; Pavone, M. Experimental and theoretical investigation on the catalytic generation of environmentally persistent free radicals from benzene. *J. Phys. Chem*. *A.* **2017**, 121 (17), 9381–9393.

(11) Thevenot, P. T.; Saravia, J.; Jin, N.; Giaimo, J. D.; Chustz, R. E.; Mahne, S.; Kelley, M. A.; Hebert, V. Y.; Dellinger, B.; Dugas, T. R.; Demayo, F. G.; Cormier, S. A. Radical-containing ultrafine particulate matter initiates epithelial-to-mesenchymal transitions in airway epithelial cells. *Am. J. Respir. Cell. Mol. Biol.* **2013**, 48 (2), 188–197.

(12) Harmon, A. C.; Hebert, V. Y.; Cormier, S. A.; Subramanian, B.; Reed, J. R.; Backes, W. L.; Dugas, T. R. Particulate matter containing environmentally persistent

541 free radicals induces AhRdependent cytokine and reactive oxygen species production
542 in human bronchial epithelial cells. *Plos. One*. **2018**, 13 (10), e0205412.
543 (13) Blakley, R. L.; Henry, D. D.; Smith, C. J. Lack of correlation between cigarette
544 mainstream smoke particulate phase radicals and hydroquinone yield*. Food. Chem.*
545 *Toxicol*. **2001**, 39 (4), 401–406.
546 (14) Khachatryan, L.; Dellinger, B. Environmentally persistent free radicals
547 (EPFRs)-2. Are free hydroxyl radicals generated in aqueous solutions?. *Environ. Sci.*
548 *Technol.* **2011**, 45 (21), 9232–9239.
549 (15) Yang, L.; Liu, G.; Zheng, M.; Jin, R.; Zhu, Q; Zhao, Y.; Wu, X.; Yang, X. Highly
550 elevated levels and particle-size distributions of environmentally persistent free
551 radicals in haze-associated atmosphere. *Environ. Sci. Technol.* **2017**, 51 (14),
552 7936–7944.
553 (16) Wang, P.; Pan, B.; Li, H.; Huang, Y.; Dong, X.; Fang, A.; Liu, L.; Wu, Min.; Xing, B.
554 The overlooked occurrence of environmentally persistent free radicals in an area
555 with low-rank coal burning, Xuanwei, China. *Environ. Sci. Technol.* **2018**, 52 (3),
556 1054–1061.
557 (17) Cormier, S. A.; Lomnicki, S.; Backes, W.; Delligner, B. Origin and health
558 impacts of emissions of toxic by-products and fine particles from combustion and
559 thermal treatment of hazardous wastes and materials. *Environ. Health*. *Perspect.*
560 **2006**, 114 (6), 810–817.
561 (18) Dellinger, B.; Lomnicki, S.; Khachatryan, L.; Maskos, Z.; Hall, R. W.;
562 Adounkpe, J.; McFerrin, C.; Truong, H. Formation and stabilization of persistent free
563 radicals. *Proc. Combust. Inst.* **2007**, 31 (1), 521–528.
564 (19) Lomnicki, S.; Truong, H.; Vejerano, E.; Delligner, B. Copper oxide-based model
565 of persistent free radical formation on combustion-derived particulate matter.
566 *Environ. Sci. Technol.* **2008**, 42 (13), 4982–4988.
567 (20) Truong, H.; Lomnicki, S.; Dellinger, B. Potential for misidentification of
568 environmentally persistent free radicals as molecular pollutants in particulate matter.
569 *Environ. Sci. Technol.* **2010**, 44 (6), 1933–1939.
570 (21) Vejerano, E.; Lomnicki, S.; Dellinger, B. Lifetime of combustion-generated
571 environmentally persistent free radicals on Zn(II)O and other transition metal oxides.
572 *J. Environ. Monit.* **2012**, 14 (10), 2803–2806.
573 (22) Patterson, M. C.; Keilbart, N. D.; Kiruri, L. W.; Thibodeaux, C. A.; Lomnicki, S.;
574 Kurtz, R. L.; Poliakoff, E. D.; Dellinger, B.; Sprunger, P. T. EPFR formation from phenol
575 adsorption on Al2O3 and TiO2: EPR and EELS studies. *Chem. Phys.* **2013**, 422,
576 277–282.
577 (23) Vejerano, E.; Lomnicki, S.; Dellinger, B. Formation and stabilization of
578 combustion-generated environmentally persistent free radicals on an Fe(III)
579 2O3/silica surface. *Environ. Sci. Technol.* **2010**, 45 (2), 589–594.
580 (24) Vejerano, E.; Lomnicki, S. M.; Dellinger, B. Formation and Stabilization of
581 Combustion-Generated, Environmentally Persistent Radicals on Ni(II)O Supported on
582 a Silica Surface. *Environ. Sci. Technol.* **2012**, 46 (17), 9406–9411.
583 (25) Chen, Q.; Wang, M.; Sun, H.; Wang, X.; Wang, Y.; Li, Y.; Zhang, L., Mu, Z.
584 Enhanced health risks from exposure to environmentally persistent free radicals and

585   the oxidative stress of PM2.5 from asian dust storms in erenhot, Zhangbei and Jinan,
586   China. *Environ. Int*. **2018**, 123, 260–268.

587   (26) Chen, Q.; Sun, H.; Mu, Z.; Wang, Y.; Li, Y.; Zhang, L.; Wang, M.; Zhang, Z.
588   Characteristics of environmentally persistent free radicals in PM2.5: Concentrations,
589   species and sources in Xi'an, Northwestern China. *Environ. Pollut.* **2019**, 247, 18–26.

590   (27) Borrowman, C. K.; Zhou, S.; Burrow. T. E.; Abbatt J. P. D. Formation of
591   environmentally persistent free radicals from the heterogeneous reaction of ozone
592   and polycyclic aromatic compounds. *Phys. Chem. Chem. Phys*. **2015**, 18 (1), 205–212.

593   (28) Tong, H.; Lakey, P. S. J.; Arangio, A. M.; Socorro, J.; Shen, F.; Lucas, K.; Brune,
594   W. H.; Pöschl, U.; Shiraiwa, M. Reactive oxygen species formed by secondary organic
595   aerosols in water and surrogate lung fluid. *Environ. Sci. Technol.* **2018**, 52 (20),
596   11642–11651.

597   (29) Chen, Q.; Sun, H.; Wang, M.; Mu, Z.; Wang, Y.; Li, Y.; Wang, Y.; Zhang, L.;
598   Zhang, Z. Dominant fraction of EPFRs from Nonsolvent-Extractable organic matter in
599   fine particulates over Xi'an, China. *Environ. Sci. Technol.* **2018**, 52 (17), 9646–9655.

600   (30) Chen, Q.; Wang, M.; Wang, Y.; Zhang, L.; Xue, J.; Sun, H.; Mu, Z. Rapid
601   determination of environmentally persistent free radicals (EPFRs) in atmospheric
602   particles with a quartz sheet-based approach using electron paramagnetic resonance
603   (EPR) spectroscopy. *Atmos. Environ.* **2018**, 184, 140–145.

604   (31) Kiruri, L.W.; Khachatryan, L.; Dellinger, B.; Lomnicki, S. Effect of copper oxide
605   concentration on the formation and persistency of environmentally persistent free
606   radicals (EPFRs) in particulates. *Environ. Sci. Technol.* **2014**, 48 (4), 2212–2217.

607   (32) Yeh, T. F.; Syu, J. M.; Cheng, C.; Chang, T. H.; Teng, H. Graphite oxide as a
608   photocatalyst for hydrogen production from water. *Adv. Funct. Mater.* **2010**, 20 (14),
609   2255–2262.

610   (33) Dabestani, R.; Ellis, K. J.; Sigman, M. E. Photodecomposition of anthracene on
611   dry surfaces: products and mechanism. *J. Photochem. Photobiol. A. Chem.* **1995**,
612   86(1), 231–239.

613   (34) Chen, Q.; Ikemori, F.; Higo, H.; Asakawa, D.; Mochida, M. Chemical structural
614   characteristics of HULIS and other fractionated organic matter in urban aerosols:
615   Results from mass spectral and FT-IR analysis. *Environ. Sci. Technol*. **2016**, 50 (4),
616   1721–1730.

617   (35) Mallakin, A.; McConkey, B.J.; Miao, G.; Mckibben, B.; Snieckus, V.; Dixon, D.G.;
618   Greenberg, B.M. Impacts of structural photomodification on the toxicity of
619   environmental contaminants: anthracene photooxidation products. *Ecotox. Environ.*
620   *Safe.* **1999**, 43, 204–212.

621   (36) Mezey, P.G.; Zimpel, Z.; Warburton, P.; Walker, P.D.; Irvine, D.G.; Huang, X.-D.;
622   Dixon, D.G.; Greenberg, B.M. Use of QShAR to model the photoinduced toxicity of
623   PAHs: Electron density shape features accurately predict toxicity. *Environ. Toxicol.*
624   *Chem.* **1998**. 17, 1207–1215.

625   (37) Huang, X.D.; McConkey, B.J.; Babu, T.S.; Greenberg, B.M. Mechanism of
626   photoinduced toxicity of photomodified anthracene to plants: inhibition of
627   photosynthesis in the aquatic higher plant Lemna gibba (Duckweed). *Environ. Toxicol.*
628   *Chem*. **1997**, 8, 1707–1715.

629   (38) Mallakin, A.; Dixon, D. G.; Greenberg, B. M. Pathway of anthracene
630   modification under simulated solar radiation. *Chemosphere*. **2000**, 40(12),
631   1435–1441.

632   (39) Krylov, S.N.; Huang, X.D.; Zeiler, L.F.; Dixon, D.G.; Greenberg, B.M.
633   Mechanistic quantitative structure-activity relationship model for the photoinduced
634   toxicity of polycyclic aromatic hydrocarbons: I. Physical model based on chemical
635   kinetics in a two-compartment system. *Environ. Toxi. Chem.* **1997**, 16 (11),
636   2283–2295.

637   (40) McNeill, K,; Canonica, S. Triplet state dissolved organic matter in aquatic
638   photochemistry: reaction mechanisms, substrate scope, and photophysical
639   properties. *Environ. Sci. Process. Impacts*. **2016**, 18, 1381–1399.

640   (41) Monge, M.E.; D'Anna, B.; Mazri, L.; Giroir-Fendler, A.; Ammann, M.;
641   Donaldson, D.J.; George, C. Light changes the atmospheric reactivity of soot. *Proc
642   Natl. Acad. Sci. USA.* **2010**, 107(15), 6605–6609.

643   (42) Dellinger, B.; Lomnicki, S.; Khachatryan, L.; Maskos, Z.; Hall, R. W.; Adounkpe,
644   J., McFerrin, C.; Truong, H. Formation and stabilization of persistent free radicals.
645   *Proc Combust Inst*. **2007**, 31(1), 521–528.

646   (43) Huang, W.; Zhang, Y.; Zhang, Y.; Zeng, L.; Dong, H.; Huo, P.; Fang, D.; Schauer,
647   J. J. Development of an automated sampling-analysis system for simultaneous
648   measurement of reactive oxygen species (ROS) in gas and particle phases: GAC-ROS.
649   *Atmos. Environ.* **2016**, 134, 18–26.

650   (44) Meulenberg, R.; Rijnaarts, H. H.; Doddema, H. J.; Field, J. A. Partially oxidized
651   polycyclic aromatic hydrocarbons show an increased bioavailability and
652   biodegradability. *FEMS Microbiol Lett*. **1997**, 152(1), 45–9.

653   (45) Nikolaou, K.; Masclet, P.; Mouvier, G. Sources and chemical reactivity of
654   polynuclear aromatic hydrocarbons in the atmosphere – A critical review. *Sci Total
655   Environ*. **1984**, 32(2), 103–132.

656   (46) Chen. L.; Zhang, Y.; Liu, B. In situ simultaneous determination the photolysis
657   of multi-component PAHs adsorbed on the leaf surfaces of living Kandelia candel
658   seedlings. *Talanta*. **2010**, 83(2), 324–331.

659   (47) Chen, Q.; Ikemori, F.; Mochida, M. Lightabsorption and
660   excitation–emissionfluorescence of urban organic aerosolcomponents and their
661   relationship to chemical structure. *Environ. Sci. Technol*. **2016**, 50(20), 10859–10868.

662   (48) Chen, Q.; Ikemori, F.; Nakamura Y.; Vodicka, P.; Kawamura, K.; Mochida, M.
663   Structural and light-absorption characteristics of complex water-insoluble organic
664   mixtures in urban submicron aerosols. *Environ. Sci. Technol*. **2017**, 51(15),
665   8293–8303.

666   (49) Gehling, W.; Khachatryan, L.; Dellinger, B. Hydroxyl Radical Generation from
667   Environmentally Persistent Free Radicals (EPFRs) in PM2.5. *Environ Sci Technol.* **2014**,
668   48(8), 4266–4272.

669   **Table 1.** The *g*-factor and ΔH_{p-p} values of the EPFRs produced by different PM

670   components and different reference materials excited by visible light.

type of sample	*g*-factor		ΔH_{p-p} (Gs)	
	range	mean ± SD	range	mean ± SD
MSOM	2.0048 - 2.0052	2.0050 ± 0.0001	7.3 - 8.0	7.7 ± 0.3
HULIS	2.0050 - 2.0054	2.0051 ± 0.0001	6.2 - 7.7	7. 2 ± 0.5
Washed sample	2.0029 - 2.0033	2.0031 ± 0.0002	5.3 - 6.9	6.2 ± 0.5
GO	2.0034 - 2.0034	2.0034 ± 0.0000	3.1 - 3.7	3.4 ± 0.3
Phenol	2.0049 - 2.0054	2.0051 ± 0.0002	6.1 - 7.1	6.5 ± 0.5
Hydroquinone	2.0052 - 2.0053	2.0052 ± 0.0001	6.5 - 8.2	7.4 ± 1.2
Resorcinol	2.0047 - 2.0048	2.0047 ± 0.0001	4.2 - 5.2	4.8 ± 0.5
2-Methyl-4-nitrophenol	2.0052 - 2.0055	2.0053 ± 0.0001	8.6 - 9.8	9.3 ± 0.6
o-Nitrophenol	2.0056 - 2.0061	2.0059 ± 0.0002	8.1 - 9.9	9.2 ± 1.0
Anthracene	2.0044 - 2.0046	2.0045 ± 0.0001	6.4 - 6.7	6.6 ± 0.1
Pyrene	2.0040 - 2.0042	2.0041 ± 0.0001	6.4 - 7.2	6.7 ± 0.4
1,4-Naphthoquinone	2.0046 - 2.0046	2.0046 ± 0.0000	5.1 - 5.6	5.3 ± 0.2
Glucose	No EPFRs were generated			
HP-WSOM				
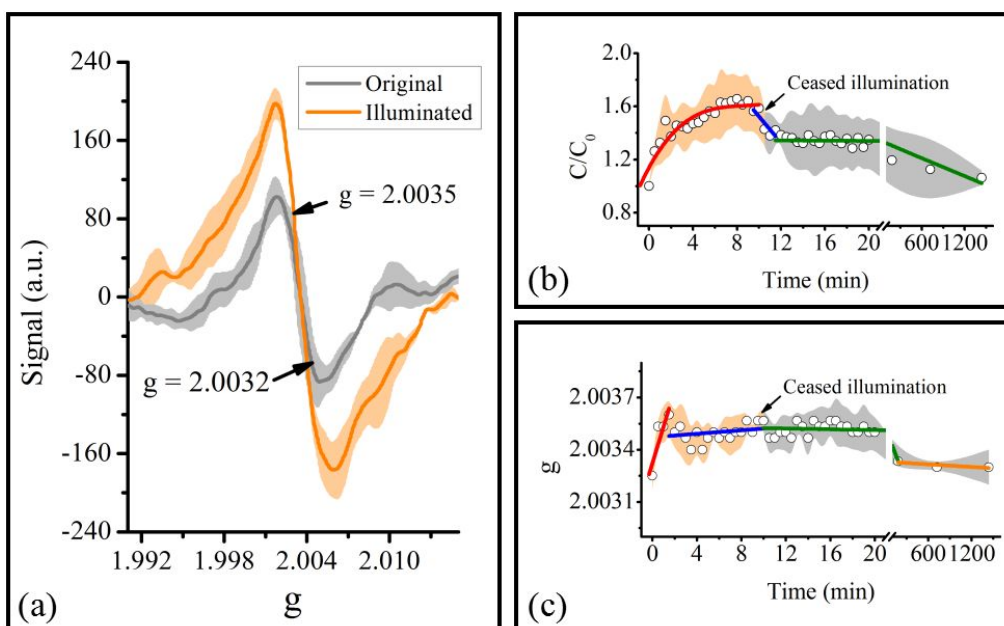
672

673 **Figure 1.** (a) Average EPR spectra of the PM$_{2.5}$ samples before and after illumination

674 (December 27-29, 2017; $n = 3$). (b) Time-varying curves of the EPFR signal intensity

675 and (c) *g*-factor during continuous illumination. The shaded area in the figure

676 represents the standard deviation range, where the yellow areas of (b) and (c)

677 represent the illumination process, the gray areas represent the nonillumination

678 process, and the lines of different colors represent different modes of variation.
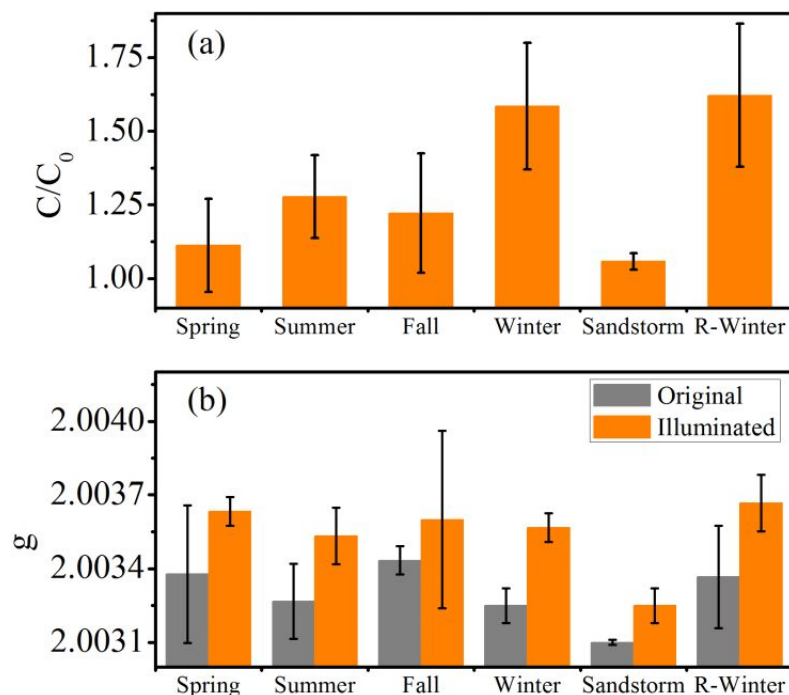
679

680   **Figure 2.** Comparison of the amounts of photochemically generated EPFRs and the

681   *g*-factors of the $PM_{2.5}$ samples in different seasons. (a) Comparison of EPFRs

682   concentration before and after illumination. C_0 represents the original concentration of

683   EPFRs, and C represents the concentration of EPFRs after illumination. (b)

684   Comparison of *g*-factor before and after illumination. Sandstorm represents the

685   sample collected under dusty weather conditions. R-Winter indicates the results of

686   repeated illumination of the winter sample (the sample is again illuminated by light

687   when EPFRs are generated by the last illumination decay).
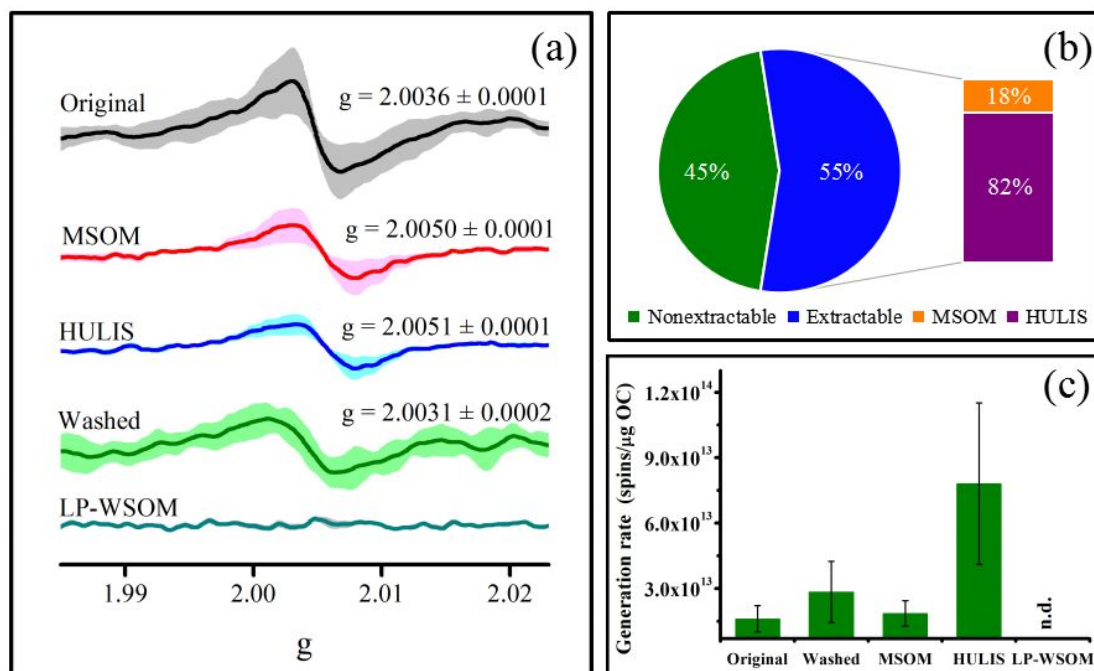
Figure 3. Secondary EPFRs produced by different PM components excited by visible light (*n* = 12). (a) The average EPR spectra of the EPFRs produced by different components. (b) The contribution ratio of each component to the overall secondary EPFRs. (c) The generation rates of the secondary EPFRs of different components. The error bars represent the standard deviation.
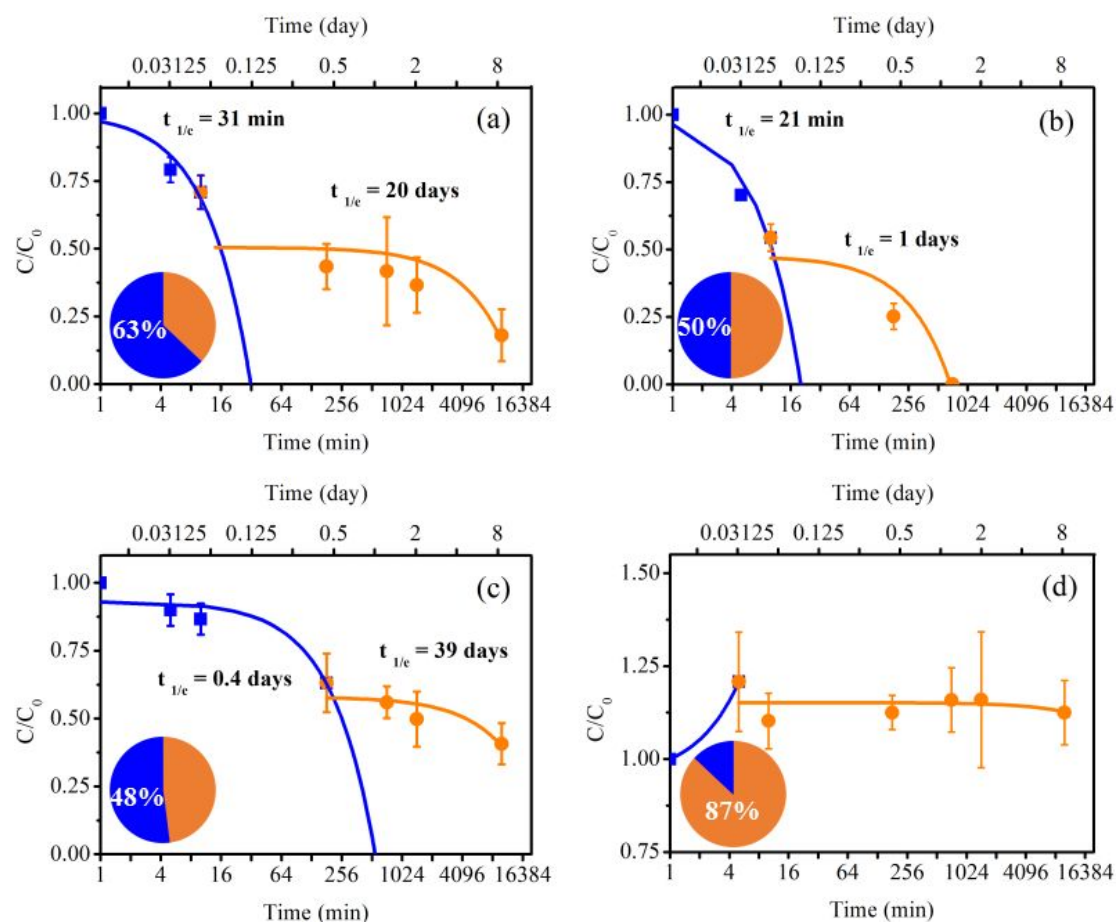
Figure 4. Secondary EPFR decay curves. (a), (b), (c) and (d) The concentrations of EPFRs generated by MSOM, phenol, anthracene and pyrene over time, respectively. Curves of different colors represent different modes of variation, and all curves are fitted with a natural exponential function. The pie charts in (a) - (c) represent the proportions of fast decay (blue) and slow decay (yellow) EPFRs. The pie chart in (d) indicates the amounts of EPFRs generated during illumination (yellow) and after illumination (blue).
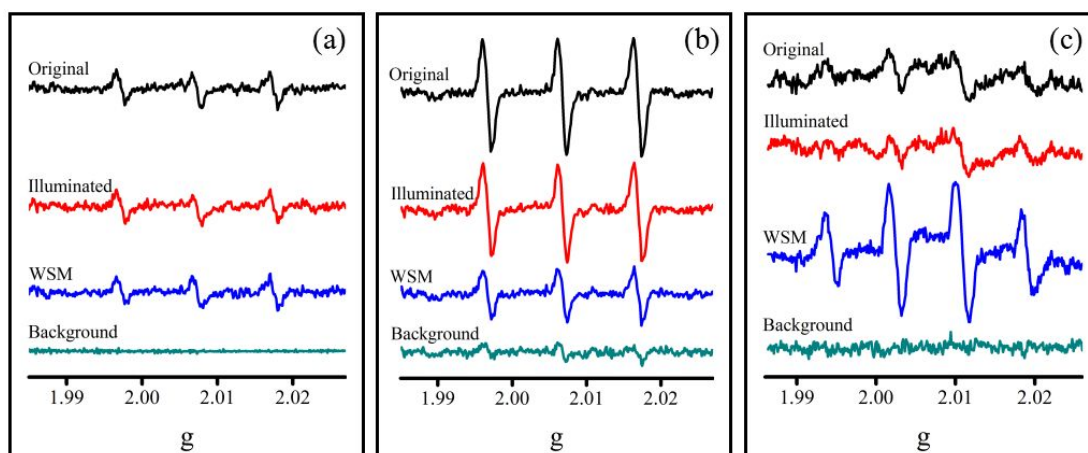
Figure 5. Average EPR spectra of $^1O_2$ and $\cdot$OH for different samples ($n = 3$). (a) and (b) The $^1O_2$ EPR spectra captured at 5 min and 24 h, respectively, after the sample is added to TEMP. (c) The EPR spectra of $\cdot$OH generated in BMPO capture samples. Original and illuminated represent the filter samples that were not illuminated and were illuminated before ROS capture experiment, respectively, and WSM represents the water-soluble material in the original sample.